

pH-Responsive Reversibly Swellable Nanotube Arrays[†]

Khek-Khiang Chia,[‡] Michael F. Rubner,^{*§,||} and Robert E. Cohen^{*‡§}

[‡]Department of Chemical Engineering and [§]Center for Materials Science and Engineering and ^{||}Department of Materials Science and Engineering, Massachusetts Institute of Technology, Cambridge, Massachusetts 02139

Received May 4, 2009. Revised Manuscript Received June 18, 2009

We demonstrate a technique for synthesizing substrate-bound arrays of submicrometer-sized reversibly swellable tubes by using porous templates. The sacrificial template approach allows straightforward control over the tube length, diameter, and lateral arrangement of the resultant surface-bound nanotubes. We also explored methods for varying the tube opening structure by altering the pore shape at the surface of the template. A specific PEM system composed of poly(allylamine hydrochloride) and poly(acrylic acid) was chosen as the building block for the nanotube arrays because of its ability to undergo pH-triggered swelling–deswelling transitions. The activation of this transition results in dramatic changes in the length and diameter of the nanotubes as characterized in situ via confocal laser scanning microscopy (CLSM). The pH-driven reversible swelling–deswelling and nanoporosity behavior observed with planar films and nanotubes of this PEM system is a direct consequence of the breaking and reforming of ionic cross-links.

Introduction

Advances have been made in the design and synthesis of nanomaterials of various shapes such as spheres,¹ tubes,² belts,³ and wires.⁴ When created in the form of surface-bound arrays and composed of materials such as carbon,² zinc oxide,⁵ peptides,⁶ and polyelectrolytes,^{1,7} such nanoscale constructs have shown potential as conductors,⁸ energy conversion devices,⁴ actuators,⁹ gecko-foot-like adhesives,¹⁰ flow sensors,¹¹ and drug-releasing agents.¹² However, the stimuli-responsiveness of surface-bound nanoarrays has seldom been explored, mostly because of the inertness of many of the materials typically utilized to create them. Of particular interest would be the ability to reversibly alter the physical and mechanical properties of nanoarrays through the use of simple triggers such as a change in solution pH or temperature.

At present, a wide range of stimuli-responsive materials, mostly in bulk form, have been designed and shown to exhibit technologically useful responses such as switchable wettability,¹³ magnetic-assisted

drug delivery,^{14,15} temperature-stimulated volume transitions,¹⁶ and photomechanical actuation.¹⁷ The synthesis of such materials in the form of nanotube/wire arrays could generate stimuli-mediated responses that may be more interesting than their bulk counterparts, owing to their high area-to-volume and length-to-diameter aspect ratios. In addition, the collective behavior of the nanotubes/wires could lead to phenomena such as an increase in compressive strength as a result of nanogranular friction and percolation effects.¹⁸

Motivated by these prospects, we fabricated reversibly swellable submicrometer-sized tubes composed of pH-responsive polyelectrolyte multilayers (PEMs) by using sacrificial porous templates.¹⁹ Sacrificial templates have been widely utilized^{20–25} for synthesizing nanotubes/wires owing to the simplicity and robustness of the process compared to other synthesis methods such as the catalytic growth method that requires careful control of the temperature and feed-to-catalyst ratio.²⁶ Additionally, the template approach allows precise control over the orientation and spacing of the resultant nanowires/tubes (identical to that of the pores on the sacrificial template), which can be challenging with other synthesis methods. As for the deposition method, various techniques have been used to deposit materials into porous templates, including sol–gel chemistry,²⁷ chemical vapor deposition,²⁸ and electroless plating,²⁹

[†] Part of the “Langmuir 25th Year: Self-assembled polyelectrolyte multilayers: structure and function” special issue.

*Corresponding authors. E-mail: rubner@mit.edu (M.F.R.), recohen@mit.edu (R.E.C.).

- (1) Wang, Y.; Angelatos, A. S.; Caruso, F. *Chem. Mater.* **2008**, *20*, 848–858.
- (2) Ebbesen, T. W.; Ajayan, P. M. *Nature* **1992**, *358*, 220–222.
- (3) Comini, E.; Faglia, G.; Sberveglieri, G.; Pan, Z. W.; Wang, Z. L. *Appl. Phys. Lett.* **2002**, *81*, 1869–1871.
- (4) Law, M.; Greene, L. E.; Johnson, J. C.; Saykally, R.; Yang, P. D. *Nat. Mater.* **2005**, *4*, 455–459.
- (5) Vayssières, L. *Adv. Mater.* **2003**, *15*, 464–466.
- (6) Hartgerink, J. D.; Grana, J. R.; Milligan, R. A.; Ghadiri, M. R. *J. Am. Chem. Soc.* **1996**, *118*, 43–50.
- (7) Ai, S. F.; Lu, G.; He, Q.; Li, J. B. *J. Am. Chem. Soc.* **2003**, *125*, 11140–11141.
- (8) Collins, P. C.; Arnold, M. S.; Avouris, P. *Science* **2001**, *292*, 706–709.
- (9) Baughman, R. H.; Cui, C. X.; Zakhidov, A. A.; Iqbal, Z.; Barisci, J. N.; Spinks, G. M.; Wallace, G. G.; Mazzoldi, A.; De Rossi, D.; Rinzler, A. G.; Jaschinski, O.; Roth, S.; Kertesz, M. *Science* **1999**, *284*, 1340–1344.
- (10) Mahdavi, A.; Ferreira, L.; Sundback, C.; Nichol, J. W.; Chan, E. P.; Carter, D. J. D.; Bettinger, C. J.; Patanavanich, S.; Chignozha, L.; Ben-Joseph, E.; Galakatos, A.; Pryor, H.; Pomerantseva, I.; Masiakos, P. T.; Faquin, W.; Zumbuehl, A.; Hong, S.; Borenstein, J.; Vacanti, J.; Langer, R.; Karp, J. M. *Proc. Natl. Acad. Sci. U.S.A.* **2008**, *105*, 2307–2312.
- (11) McConney, M. E.; Chen, N.; Lu, D.; Hu, H. A.; Coombs, S.; Liu, C.; Tsukruk, V. V. *Soft Matter* **2009**, *5*, 292–295.
- (12) Kohli, P.; Martin, C. R. *Curr. Pharm. Biotechnol.* **2005**, *6*, 35–47.
- (13) Xia, F.; Feng, L.; Wang, S. T.; Sun, T. L.; Song, W. L.; Jiang, W. H.; Jiang, L. *Adv. Mater.* **2006**, *18*, 432–436.
- (14) Hafezi, U. O. *Magnetically modulated therapeutic systems*; Elsevier Science Bv: 2004, pp 19–24.

(15) Son, S. J.; Reichel, J.; He, B.; Schuchman, M.; Lee, S. B. *J. Am. Chem. Soc.* **2005**, *127*, 7316–7317.

(16) Chu, L. Y.; Niitsuma, T.; Yamaguchi, T.; Nakao, S. *AIChE J.* **2003**, *49*, 896–909.

(17) Ahir, S. V.; Terentjev, E. M. *Nat. Mater.* **2005**, *4*, 491–495.

(18) Tai, K.; Ulm, F. J.; Ortiz, C. *Nano Lett.* **2006**, *6*, 2520–2525.

(19) Martin, C. R. *Science* **1994**, *266*, 1961–1966.

(20) Liang, Z. J.; Susha, A. S.; Yu, A. M.; Caruso, F. *Adv. Mater.* **2003**, *15*, 1849–1853.

(21) Yan, C. L.; Liu, J.; Liu, F.; Wu, J. S.; Gao, K.; Xue, D. F. *Nanoscale Res. Lett.* **2008**, *3*, 473–480.

(22) Rohan, J. F.; Casey, D. P.; Ahern, B. M.; Rhen, F. M. F.; Roy, S.; Fleming, D.; Lawrence, S. E. *Electrochem. Commun.* **2008**, *10*, 1419–1422.

(23) Suber, L.; Imperatori, P.; Ausanio, G.; Fabbri, F.; Hofmeister, H. *J. Phys. Chem. B* **2005**, *109*, 7103–7109.

(24) Mueller, R.; Daehne, L.; Fery, A. *J. Phys. Chem. B* **2007**, *111*, 8547–8553.

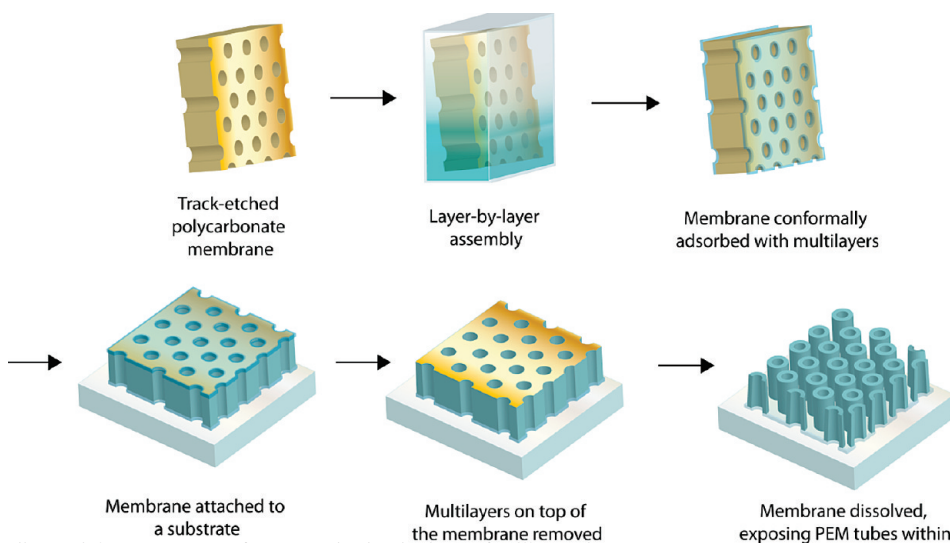
(25) Tian, Y.; He, Q.; Tao, C.; Li, J. B. *Langmuir* **2006**, *22*, 360–362.

(26) Wen, X. G.; Wang, S. H.; Ding, Y.; Wang, Z. L.; Yang, S. H. *J. Phys. Chem. B* **2005**, *109*, 215–220.

(27) Lakshmi, B. B.; Patrissi, C. J.; Martin, C. R. *Chem. Mater.* **1997**, *9*, 2544–2550.

(28) Shen, X. P.; Liu, H. J.; Fan, X.; Jiang, Y.; Hong, J. M.; Xu, Z. *J. Cryst. Growth* **2005**, *276*, 471–477.

(29) Yabu, H.; Hirai, Y.; Shimomura, M. *Langmuir* **2006**, *22*, 9760–9764.

Scheme 1. Synthesis of Surface-Bound PEM Tube Arrays^a

^a An idealized periodic spatial arrangement of pores and tubes is shown for illustration purposes.

the layer-by-layer technique was chosen because it provides a promising approach for preparing PEMs with specific physical and chemical properties, including pH-triggered reversible swellability. In addition, the ability to create complex multimaterial heterostructures with nanoscale control over dimensions is readily achievable with this approach.

To our knowledge, the reversible swellability of stimuli-responsive PEM nanotube arrays has not been reported in literature. In this work, we chose a PEM system composed of poly(allylamine hydrochloride) (PAH) and poly(acrylic acid) (PAA) that has been shown previously to undergo pH-induced, reversible nano- and microporosity transitions. We demonstrate that large dimensional changes in the surface-bound nanotubes (approaching 520% volumetric expansion) can be triggered by swelling–deswelling transitions, possibly leading to applications such as mechanical actuation, controlled drug release, and pH sensors.

Experimental Section

Materials. Poly(allylamine hydrochloride) (PAH, M_w 70 000, Sigma-Aldrich) and poly(fluorescein isothiocyanate allylamine hydrochloride) (FITC-PAH, M_w 15 000, Sigma-Aldrich) were used as polycations whereas poly(acrylic acid) (PAA, M_w 90 000, 25% aqueous solution, Polysciences) are used as the polyanion. All polyelectrolytes were used as received without further purification. PAH and PAA were prepared as 10^{-2} M solutions (based on the repeat-unit molecular weight), and FITC-PAH was prepared as a 0.5 g/L solution, all in ultrapure 18 MΩ cm deionized water (Millipore Milli-Q). The polyelectrolyte solutions were adjusted to the desired pH (± 0.01) with 1 M HCl or 1 M NaOH. The templates used during PEM assembly were track-etched polycarbonate (TEPC) membranes (Whatman) that have a thickness of ca. 10 μm and a variety of pore sizes. Amine-treated glass slides (Sigma-Aldrich) were used as substrates for affixing the template prior to membrane dissolution. Carboxylate-modified, fluorescent-red polystyrene beads (2.0 μm, Sigma-Aldrich) were used for mechanical actuation studies.

PEM Assembly and Characterization. PEMs were assembled by immersing a substrate into a polycation solution (PAH or FITC-PAH) for 15 min, followed by three water rinsing steps (2, 1, and 1 min) using a programmable slide stainer (Zeiss). FITC-PAH was used only for synthesizing tubes to be imaged with confocal laser scanning microscopy (CLSM). The substrates can be either glass slides (for assembling flat films) or TEPC membranes (for synthesizing tube arrays). The substrates were

then immersed in a polyanion solution (PAA) for 15 min, followed by identical rinsing steps. A PEM notation of (PolyA x /PolyB y) $_z$ is used, where PolyA represents the first polyelectrolyte adsorbed onto the substrate, its assembly pH, x , the second polyelectrolyte, PolyB, its assembly pH, y , and the total number of bilayers, z . All PEMs were processed and characterized right after film assembly. Film thickness was measured using a J. A. Woollam Co., Inc. VASE spectroscopic ellipsometer. In some cases where the film was in contact with a selected aqueous solution, the film thickness was measured *in situ* using a quartz cell. Data were collected between 300 and 1000 nm at a 70° angle of incidence and were analyzed with the WVASE32 software package, fitted with a Cauchy model, which assumes the real part of the refractive index, n_f , as a function of wavelength, λ , to be $n_f(\lambda) = A_n + (B_n/\lambda^2) + (C_n/\lambda^4)$ where A_n , B_n , and C_n are constants. The extent of swelling of the PEMs in solution was defined as

$$\text{extent of swelling} = \frac{\text{film thickness in solution} - \text{film thickness in dry state}}{\text{film thickness in dry state}} \times 100\%$$

Tube Array Synthesis and Characterization. After PEM assembly, the TEPC membrane was wetted with DI water, placed on an amine-treated glass substrate (which has positive residual surface charges), and heated in an oven at 60 °C for 15 min to enhance electrostatic adhesion between the PEM and the glass substrate. The unattached side of the membrane was then plasma etched (Harrick Scientific Plasma Cleaner) in oxygen at 150 mTorr for 15 min, which selectively removed the flat film deposited on the membrane surface. The entire sample was then immersed four times in fresh dichloromethane (Sigma-Aldrich) for 20, 2, 2, and 1 min. The dry PEM tube arrays were imaged with a high-resolution scanning electron microscope (JEOL 6320 HR-SEM). A CLSM (Zeiss LSM 510) was used for *in situ* imaging in water. To allow water to penetrate through the tubes more easily, a small amount of ethanol (ca. 100 μL) was dropped onto the tubes prior to imaging. In the mechanical actuation studies reported below, the tubes were immersed in a suspension of fluorescent-red carboxylate-modified polystyrene beads (Sigma-Aldrich) for 10 min prior to imaging under the aqueous conditions. For illustration purposes, we often construct plan- or side-view images from CLSM by combining the data from all scan heights using the maximum function (the maximum channel values for all nontransparent pixels) in Adobe Photoshop CS3.

Results and Discussion

In previous work from our laboratory, submicrometer-sized PEM tubes were produced as free suspensions in solvents by using template-based synthesis techniques.³⁰ Others have also prepared PEM tubes by using this approach,^{7,20,24,25,31–35} however, to our knowledge, all literature to date describes PEM nanotubes that are completely detached from a surface and characterized in suspension or after being collected on a substrate. A typical scheme involves (i) the deposition of the desired material onto a porous template, (ii) the removal of materials residing on the template surfaces to allow complete detachment of the tubes from each other upon template dissolution, and (iii) the dissolution of the template, which releases the newly created nanoelements into the solvent. The nanotubes lose their original orientation and spatial arrangement when suspended in a solution or collected on a substrate.

In this work, the tube arrays were affixed to a substrate, thereby allowing them to retain the negative image of the template and providing the possibility to (i) control the orientation and spatial configuration of the tubes and (ii) study the collective behavior of the tubes with specific orientations and spatial configurations. To do so, only one side of the PEM film residing on the template surfaces was removed, and the other side was attached to a substrate. Preservation of the film on the other side of the template allows the base of the tubes to be fixed in place, which is crucial in maintaining the original orientation and spatial configuration of the tube arrays.

The overall synthesis scheme is summarized in Scheme 1 and involves (i) layer-by-layer assembly of polyelectrolytes that conformally deposit onto the template, both on the surfaces and in the pores, (ii) template attachment to a substrate, (iii) plasma etching on the unattached side of the template for selective PEM removal at that surface, and (iv) template dissolution in dichloromethane. Commercially available track-etched polycarbonate (TEPC) membranes were used in this study to capitalize on the compatibility of typical polycarbonate solvents (e.g., dichloromethane) with the PAH7.5/PAA3.5 PEM system. Certain membranes, such as those made of anodized alumina, dissolve only at extremely high or low pH values that can disassemble the PAH/PAA PEM. The choice of the TEPC membrane was not ideal for the purpose of synthesizing perfectly aligned or laterally arranged tubes because of the random pore arrangement produced by particle bombardment during membrane production. Thus, as expected, tube arrays with the same irregular orientations and spatial arrangements (Figure 1) as the pore structure of the membranes were observed. Studies are underway to develop templates with controlled pore orientations and spatial arrangements using materials that dissolve in solvents compatible with the PEM system.

Variation of Tube Size and Shape via Template Alteration. As mentioned earlier, the use of a sacrificial template results in the formation of tubes with shapes and dimensions similar to those of the pores; the tube diameter can therefore be controlled directly by varying the pore size and the number of deposited multilayers. To demonstrate this, TEPC membranes with different pore sizes (0.4, 0.8, and 3.0 μm) were deposited with the same number of PAH7.5/PAA3.5 bilayers, resulting in the formation of tubes with diameters similar to the original template pore sizes (Figure 1). As evident from the scanning electron microscopy (SEM) images, with

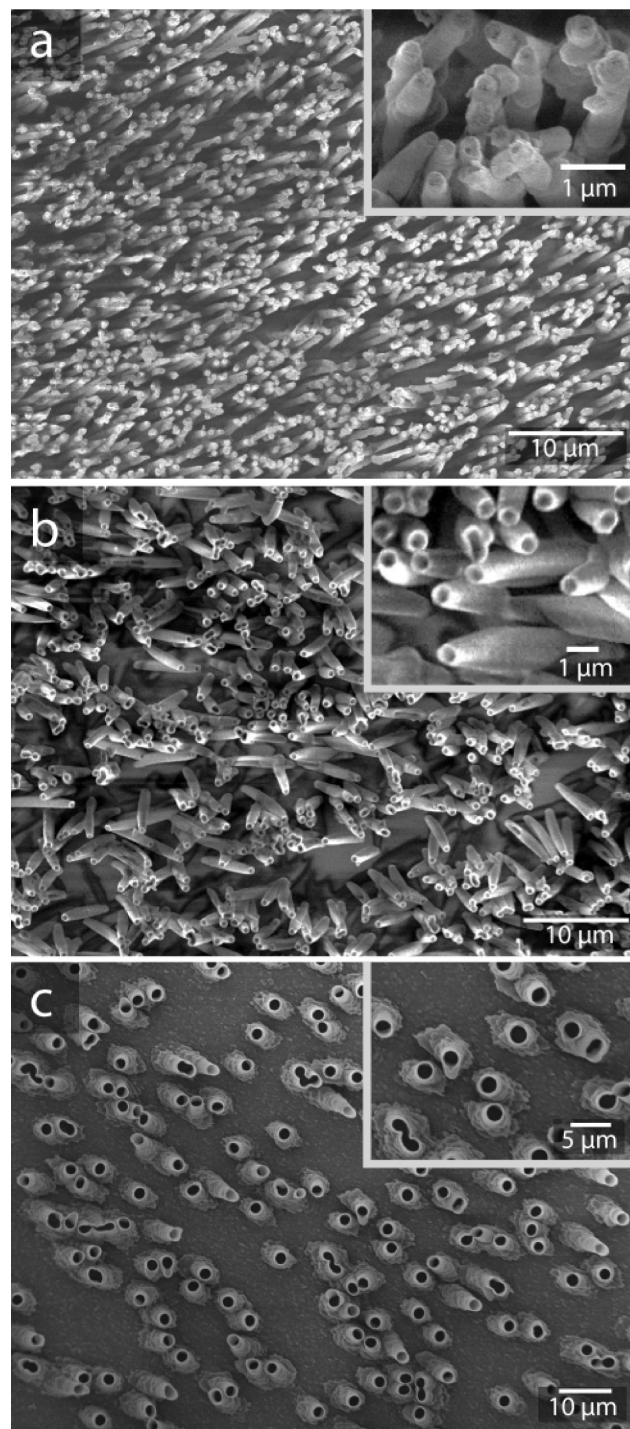


Figure 1. SEM images of $(\text{PAH7.5}/\text{PAA3.5})_{20}$ PEM tube arrays synthesized with TEPC membranes with pore sizes of (a) 0.4, (b) 0.8, and (c) 3.0 μm . Membranes were attached to a substrate with the glossy side facing up. Images were collected after drying of the template-dissolving solvent. (Inset) Higher magnification.

the same number of bilayers (and thus wall thickness), the tubes could be hollow or essentially filled (at least as observed from the tip of the tubes) depending on the template pore size.

Apart from their length and diameter, control over the opening structure of the nanotubes is particularly valuable because this would be expected to influence important surface properties such as wettability. Without alterations of the TEPC membranes, the opening structure of the nanotubes was observed to be different depending on the side of the membrane attached to the substrate.

(30) Lee, D.; Cohen, R. E.; Rubner, M. F. *Langmuir* **2007**, *23*, 123–129.
 (31) He, Q.; Song, W.; Möhwald, H.; Li, J. *Langmuir* **2008**, *24*, 5508–5513.
 (32) He, Q.; Tian, Y.; Cui, Y.; Mohwald, H.; Li, J. *J. Mater. Chem.* **2008**, *18*, 748–754.
 (33) Cepak, V. M.; Martin, C. R. *Chem. Mater.* **1999**, *11*, 1363–1367.
 (34) Cuenot, S.; Alem, H.; Louarn, G.; Demoustier-Champagne, S.; Jonas, A. M. *Eur. Phys. J. E* **2008**, *25*, 343–348.
 (35) Yu, A.; Liang, Z.; Caruso, F. *Chem. Mater.* **2005**, *17*, 171–175.

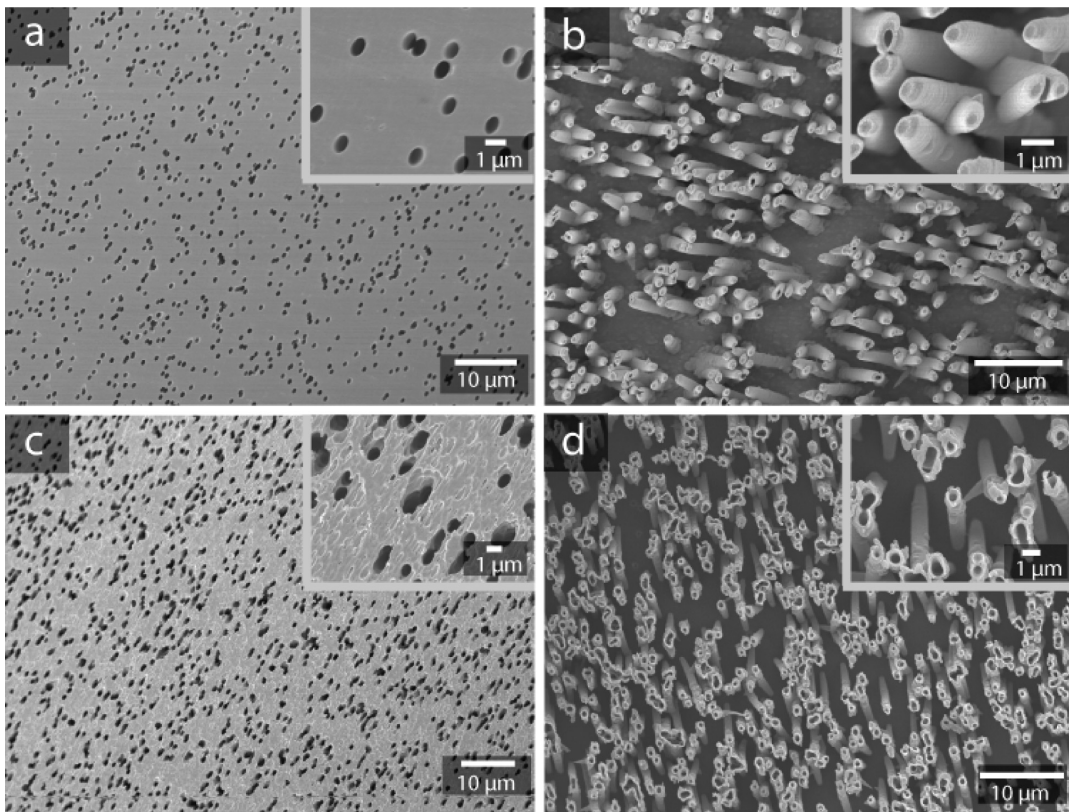


Figure 2. SEM images of (a) the glossy side of the $0.8\text{ }\mu\text{m}$ TEPC membrane and (b) the resulting tubes; (c, d): similar to images a and b except using the matte side of the membrane. (Inset) Higher magnification.

As shown in Figure 2, opening shapes that were either tapered in or fluted out could be obtained by simply changing the side of the template that was attached to the substrate. SEM images revealed two distinct surface features of the TEPC membranes: one side that is smooth with relatively straight projected holes (Figure 2a) and the opposite side that is rougher with holes that taper out at the template surface (Figure 2c). The surface with better defined exit holes is glossy, whereas the opposite surface has a matte finish. The difference in surface features is probably a result of an “entrance effect” created during particle bombardment of the membrane. As expected, placing the glossy side up led to tubes that were tapered in with smaller diameters whereas tubes formed with the matte side up exhibit a fluted shape with larger opening diameters. These seemingly small differences were significant enough to alter the wettability of the tube arrays. With either tube-opening structure, dry PEM tube arrays (dried from solvent) were water repellent as a result of the composite air–solid interface established by the nanotube forest, but advancing water droplet contact angles were consistently higher for tube arrays with the fluted opening structure (137 vs 125°) because the composite air–solid interface was able to support a larger water droplet without wetting. This effect may prove useful in the design of surface arrays with tunable wetting characteristics.

To enhance the water repellency of these PEM nanotube arrays further, the pore openings on the matte side surface were expanded by plasma etching. The plasma-etched membrane was then deposited with PEMs, followed by the same membrane attachment and dissolution procedures. Membranes plasma etched with oxygen for 30 min ultimately led to tube arrays with a much more fluted opening structure (Figure 3). This array of tubes showed static, advancing, and receding contact angles (VCA-Optima 2000 instrument) of 153 , 150 , and 135° , respectively.

Choice of PEM System as the Building Block for Stimuli-Responsive Nanotube Arrays. The PAH_{7.5}/PAA_{3.5} multilayer

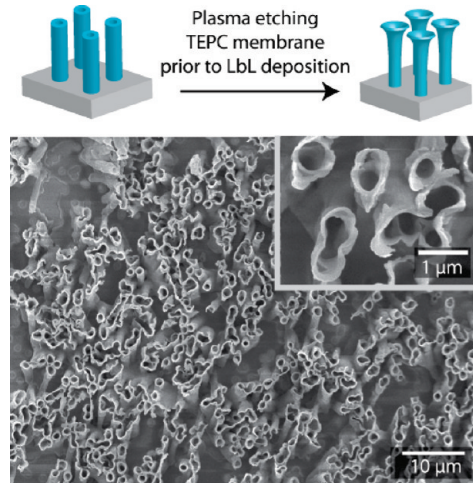


Figure 3. (Top) Three-dimensional cartoon rendering of PEM tubes synthesized without alterations on the TEPC membrane vs those synthesized with plasma etching of the TEPC membrane prior to layer-by-layer deposition. (Bottom) SEM image of the resulting $(\text{PAH7.5}/\text{PAA3.5})_{20}$ PEM tubes following the latter procedure. (Inset) Higher magnification.

was pursued as a stimuli-responsive system on the basis of previous work^{36–39} that found that it and related multilayers, PAH_{8.6}/PAA_{3.5}, demonstrated an ability to undergo micro- and

(36) Hiller, J.; Mendelsohn, J. D.; Rubner, M. F. *Nat. Mater.* **2002**, *1*, 59–63.

(37) Mendelsohn, J. D.; Barrett, C. J.; Chan, V. V.; Pal, A. J.; Mayes, A. M.; Rubner, M. F. *Langmuir* **2000**, *16*, 5017–5023.

(38) Zhai, L.; Cebeci, F. C.; Cohen, R. E.; Rubner, M. F. *Nano Lett.* **2004**, *4*, 1349–1353.

(39) Zhai, L.; Nolte, A. J.; Cohen, R. E.; Rubner, M. F. *Macromolecules* **2004**, *37*, 6113–6123.

nанопористые переходы после различных обработок pH. В предыдущем исследовании было обнаружено, что нанопоры^{36,39} в сухом состоянии могут быть обратимо открыты и закрыты при соответствующих обработках pH в влажном состоянии. Возможность создания нанотрубок с пористыми структурами на внутренней поверхности изначально мотивировала исследование этого многослойного систем; однако, как будет ясно из дальнейшего изложения, PAH7.5/PAA3.5 многослойные системы демонстрируют широкий спектр интересных стимули-чувствительных эффектов.

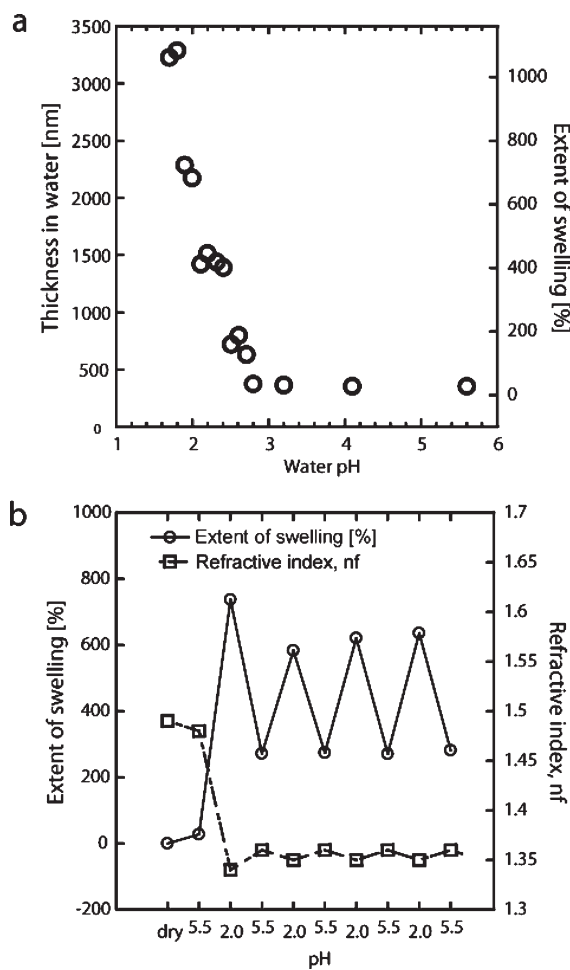


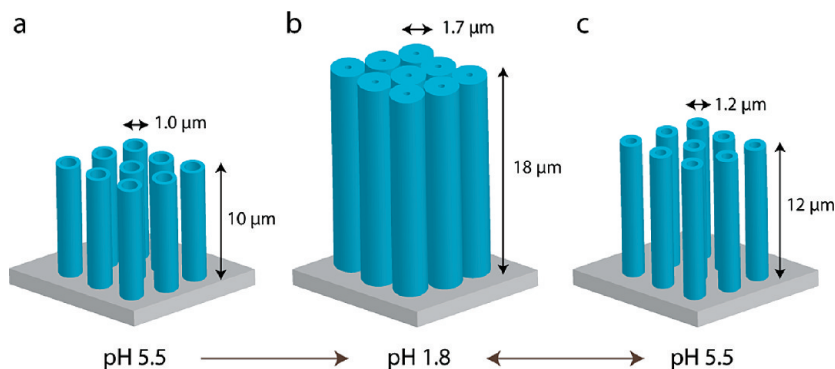
Figure 4. In situ ellipsometry measurements of (a) the film thickness and extent of swelling of (PAH7.5/PAA3.5)₂₀ PEMs immersed in water at different pH values and (b) the extent of swelling and effective refractive index of a multilayer film immersed sequentially in water at pH 5.5 and 2.0.

To gain insight into what occurs during the different pH treatments used to activate the opening and closing of nanopores, film thicknesses (measured on multilayers supported on planar substrates) were measured *in situ* as a function of the surrounding solution pH by using ellipsometry. Although in a previous study it was found³⁶ that low-pH treatments (≤ 2.0) closed the nanopores observed in the dry state whereas high-pH treatments (≥ 5.5) opened the pores, a detailed investigation of the wet-state behavior of this multilayer system was not reported. *In situ* ellipsometry measurements (Figure 4a) reveal that the thickness of the multilayer film remained constant in the higher-pH range and started to increase only below pH 2.5. At lower pH, the degree of swelling increases dramatically until pH 1.8, below which the multilayer disassembles. The thicknesses reported at the lowest pH values represent an upper-limit estimate because the refractive index of the multilayer in this highly hydrated state became very close to that of water. This dramatic swelling transition is essentially reversible as long as the solution pH is not dropped below 1.8.

It is interesting that the reversibility and magnitude of the swelling transition indicates that the change from a porous to nonporous dry state may not be a simple carboxylate/carboxylic acid-driven process involving the opening and closing of carboxylic acid-lined pores created during the initial low-pH treatment as previously speculated.³⁶ Clearly, the presence of a reversible swelling transition shows that whatever multilayer structure is created by a subsequent high-pH treatment is erased at low pH by the breaking of ionic bonds (full mechanism to be discussed below). The swelling and deswelling transitions of the PAH7.5/PAA3.5 film were reversible for at least four cycles (Figure 4b), making it a useful candidate as the building block for stimuli-responsive nanotube arrays.

Stimuli-Responsive Nanotube Arrays. Confocal laser scanning microscopy (CLSM) was used to characterize the swelling transition of nanotube arrays fabricated from PAH7.5/PAA3.5 multilayers. Fluorescently labeled PAH was used to provide imaging contrast. Using a 40 \times water immersion objective lens, plan-view images of the tube arrays were collected at each scan height and stacked using the maximum function in Adobe Photoshop. Compiled plan-view and side-view images of the tube arrays immersed in water at different pH values are shown in Figure 5, with their corresponding 3-D cartoon renderings shown in Scheme 2. Figure 5a shows PEM tubes immersed in water at pH 5.5 with dimensions similar to those of the dry tube arrays characterized by SEM (Figure 1). When immersed in water at pH 1.8, the nanotubes swelled substantially in both the vertical and horizontal directions (Figure 5b and Scheme 2), essentially filling much of the space between tubes. In the highly swollen state, the

Scheme 2. Three-Dimensional Cartoon Renderings Illustrating the Dimensional Changes of the Tube Arrays Immersed in Solutions with Different pH Values



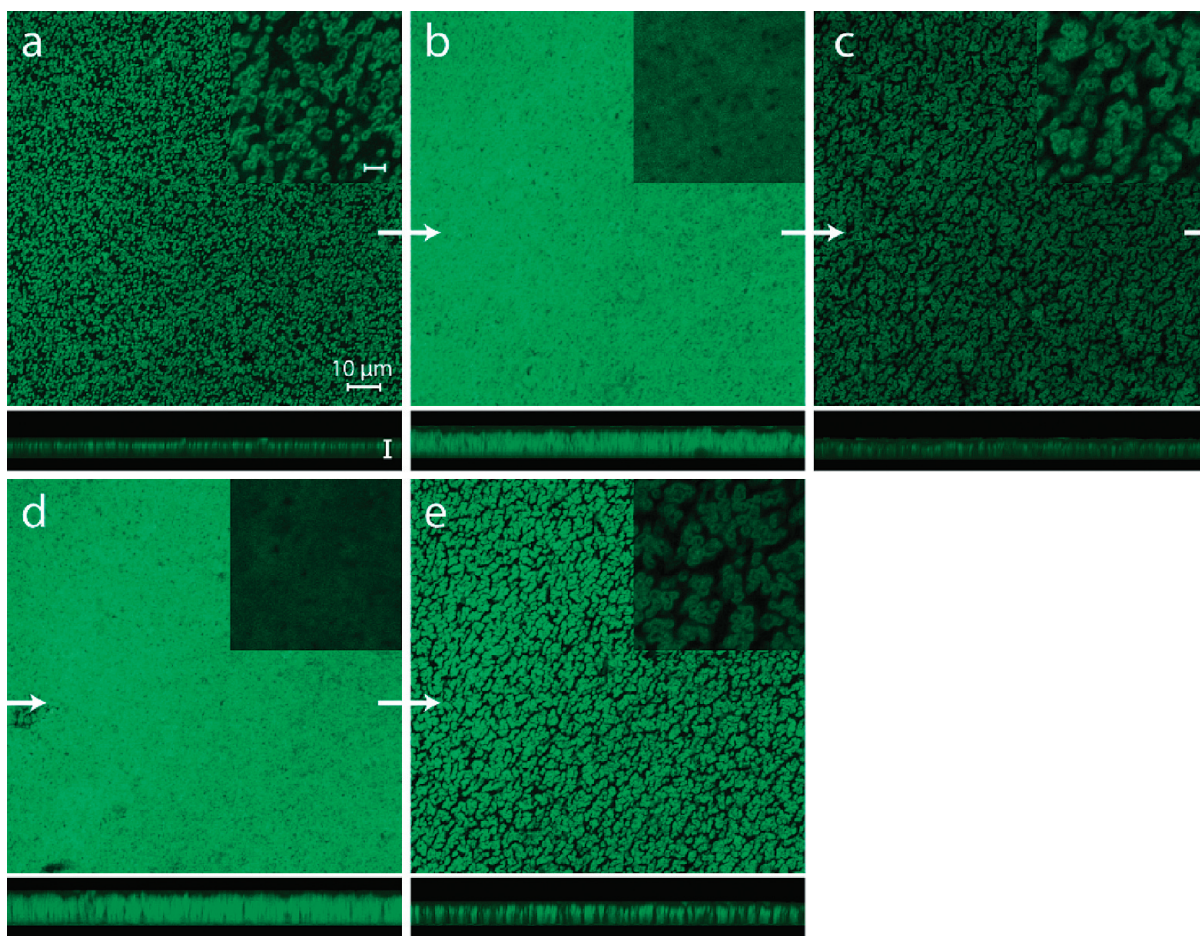


Figure 5. Confocal laser scanning microscopy (CLSM) plan-view images of $(\text{PAH7.5}/\text{PAA3.5})_{20}$ tube arrays sequentially immersed in water at pH 5.5 (a, c, e) and 1.8 (b, d). (Inset) Higher magnification. (Below) Side-view image. All images were constructed by compiling scans at different sample heights and stacking them with the maximum function. Scale bars: 10 μm .

outer diameter and length of the nanotubes increased from 1.0 to 1.7 μm and 10 to 18 μm , respectively. Even in the highly swollen state, however, the tubes remained intact as individual tubes without dissociating completely or merging irreversibly with surrounding tubes, as observed from the pH cycles shown in Figure 5 and higher-magnification images shown in Figure 6. When the pH is increased to 5.5, the tube dimensions decreased but are somewhat larger than the original values (height = 12 μm , diameter = 1.2 μm). This type of swelling–deswelling behavior was also consistently observed in studies of films assembled on planar substrates (Figure 4b). Thus, the swelling–deswelling transition of the PEM nanotubes was essentially repeatable for at least a few cycles.

Mechanical Actuation of Colloidal Particles by Nanotube Arrays. The significant changes in nanotube diameter and length associated with the reversible swelling–deswelling transition provide a means to create simple pH-controlled mechanical actuators. To demonstrate this, a small amount of carboxylate-modified, fluorescent-red polystyrene (PS) colloidal particles (2.0 μm size) was adsorbed onto the nanotube arrays prior to CLSM imaging in DI water (pH 5.5). The particle-bound nanotube arrays were then alternately immersed in water at pH 5.5 and 1.8; the resultant constructed plan-view images (multiple plan-view images stacked using the maximum function in Adobe Photoshop) are shown in Figure 7. Using the same method, side-view images were also constructed to show more clearly the change in location of the PS particles that occurs when the

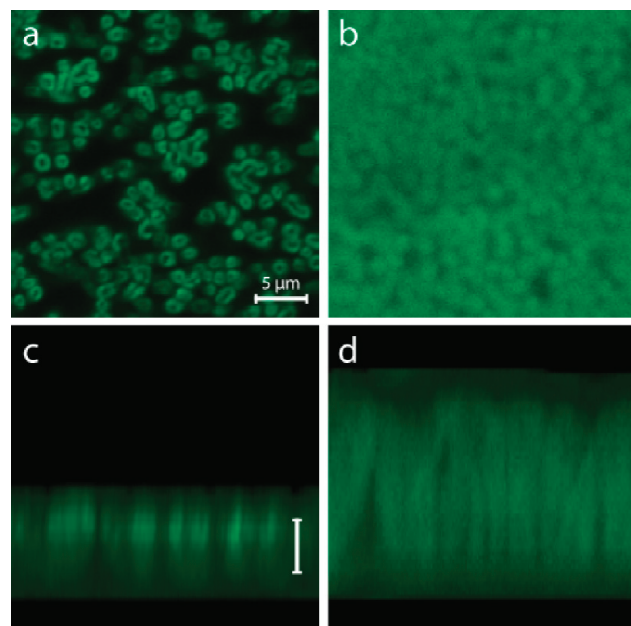


Figure 6. (a, b) Higher-magnification plan-view CLSM images of $(\text{PAH7.5}/\text{PAA3.5})_{20}$ tube arrays immersed in water at pH 5.5 and 1.8, respectively. Both images were scanned at half tube length (not compiled from multiple scans at different heights). (c, d) Compiled side-view images of panels a and b, respectively. Scale bars: 5 μm .

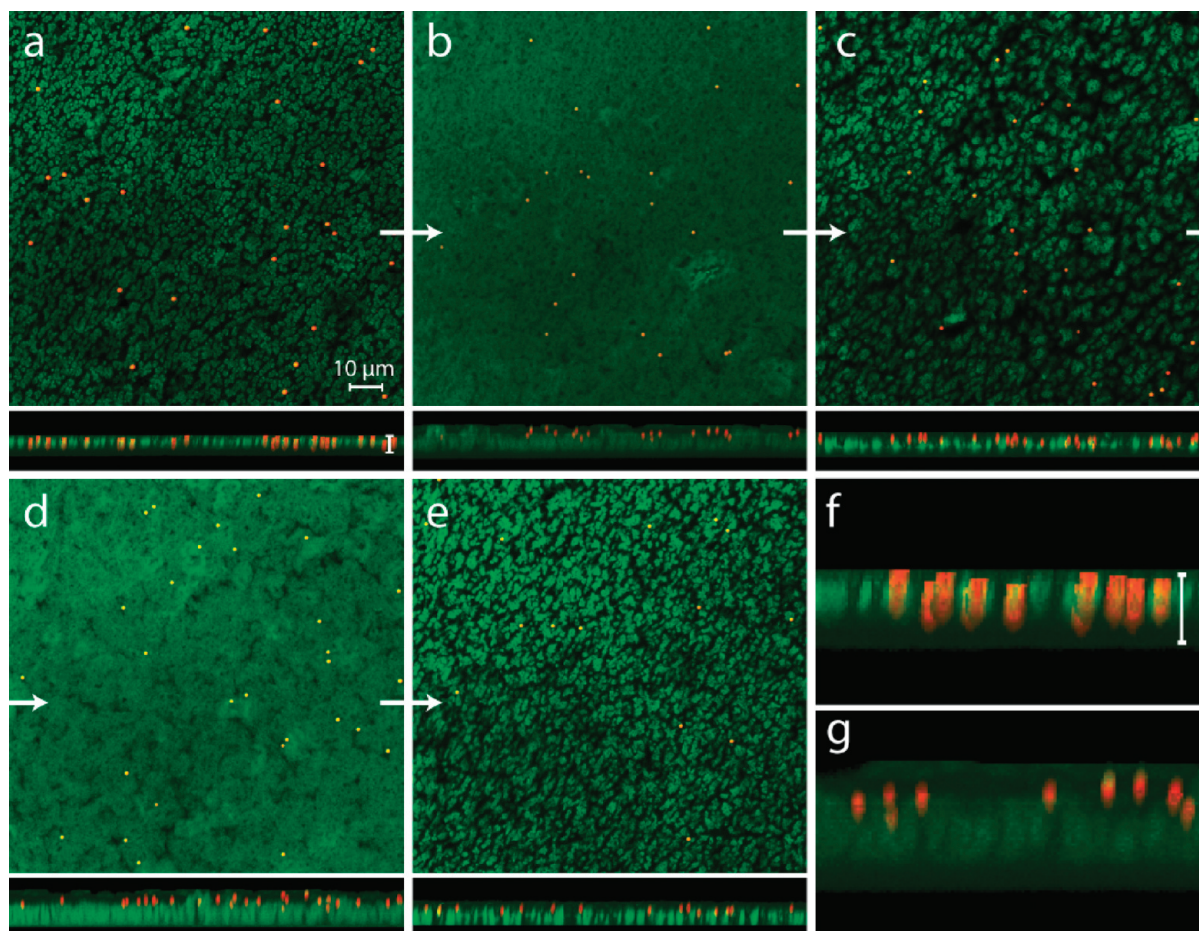


Figure 7. (a–e) CLSM plan-view images of $(PAH7.5/PAA3.5)_{20}$ tube arrays lightly decorated with $2.0\ \mu m$ fluorescent-red polystyrene particles. The sample was sequentially immersed in water at pH 5.5 (a, c, e) and 1.8 (b, d). (Below) Side view of the nanotube arrays. (f, g) Magnified side-view images from a and b, respectively. Images were compilations from scans at different sample heights and were stacked with the maximum function. Scale bars: $10\ \mu m$.

nanotubes change their dimensions. When immersed in water at pH 5.5, the spherical PS particles are oval with a Gaussian-like distribution of fluorescence intensity in the vertical direction (Figure 7f), implying vertical movement of the PS particles during movement of the sample stage between each height scan. (The side-view images are compilations of multiple images scanned with vertical stage movements.) This apparent mobility of the PS particles suggests that they are only loosely bound to the nanotubes at pH 5.5. When immersed in water at pH 1.8, the particles appear to be more spherical (Figure 7g), signifying a more highly constrained mobility. At this low pH, the nanotubes contain an excess of positively charged amine groups (to be discussed), producing stronger electrostatic binding of the negatively charged colloidal particles.⁴⁰ This electrostatic effect, however, would be mediated by the lower charge density of the PS particles that is also anticipated at this lower pH. The mobility of the PS colloidal particles is also likely to be physically/sterically limited by the highly swollen network of nanotubes. Subsequent immersion in water at pH 5.5 deswelled the tubes and moved the colloidal particles back to their original position relative to the substrate surface. This process is reversible through cycles of high- and low-pH treatments, demonstrating the ability of the

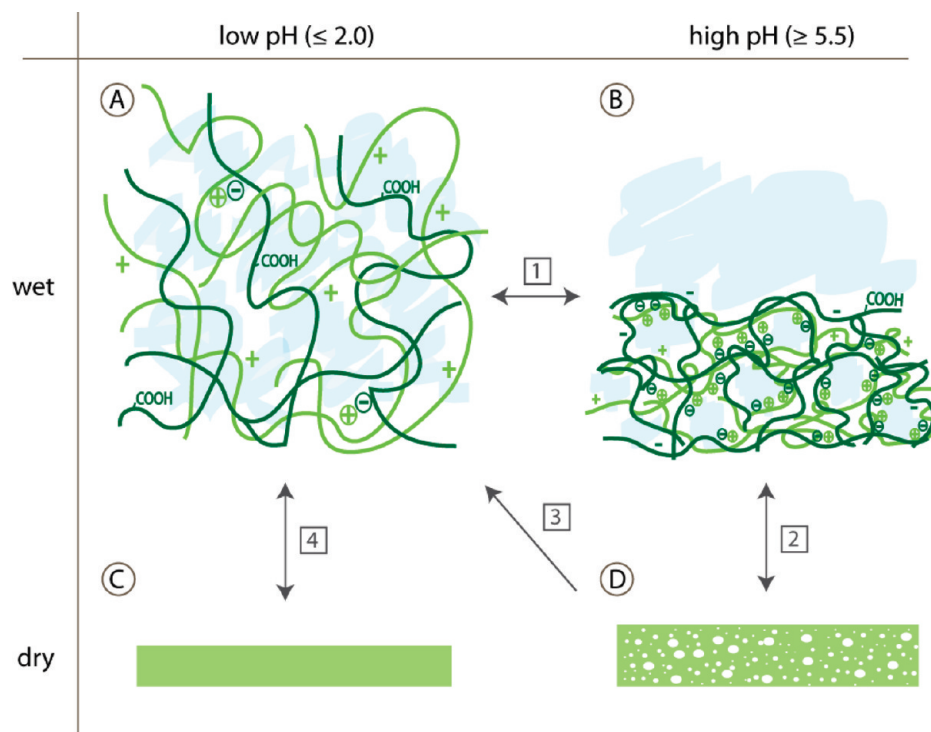
stimuli-responsive nanotube arrays to actuate the PS particles reversibly and change their binding affinities.

Mechanism of the Stimuli-Responsive Behavior and Relation to Nanoporosity Transition. To explain the full suite of stimuli-responsive properties exhibited by PAH7.5/PAA3.5 multilayers in the form of both planar films and nanotube arrays, it is necessary to take into account both the pH-induced swelling–deswelling and porosity transitions in the wet and dry states, respectively. The porosity transition is clearly a consequence of what occurs in the solution state. Previously it was found that, after an initial low-pH treatment (≤ 2.0), PAH7.5/PAA3.5 and related multilayers could be rendered reversibly nanoporous by subsequent pH treatments.³⁶ Specifically, it was found that drying from a pH 1.8 solution produced a dense, nonporous film whereas shifting the solution pH upward followed by drying from a pH 5.5 solution produced a thicker, low refractive index, nanoporous film.

In this work, *in situ* studies in water of both nanotube arrays and planar films reveal that a significant reversible swelling transition occurs at a low pH. It has previously been suggested that treating an as-assembled PAH7.5/PAA3.5 multilayer at low pH (≤ 2.0) breaks polymer–polymer ionic cross-links by protonating a significant fraction of the carboxylate groups of PAA, thereby allowing the multilayer to reorganize into a structure that can undergo a reversible porosity transition.^{36,37} These new *in situ* results show that the breaking of these ionic cross-links induces a

(40) Chia, K.-K.; Cohen, R. E.; Rubner, M. F. *Chem. Mater.* **2008**, *20*, 6756–6763.

Scheme 3. (A, B) Proposed Molecular Arrangements of the Polymers in a PAH7.5/PAA3.5 Multilayer Film in High- and Low-pH Solutions and (C, D) Morphology of the Films upon Drying



dramatic swelling transition that can be reversed by simply increasing the solution pH above the swelling–deswelling trigger point of pH 2.5. Recent results help to provide insight into the underlying mechanism of this swelling transition.⁴⁰

In DI water (pH ~5.5), as-assembled $(\text{PAH7.5/PAA3.5})_{20}$ multilayers swell by ca. 40%, with the thickness and refractive index (n_f) values of planar films changing from 200 to 280 nm and 1.51 to 1.48 respectively. When immersed in a lower-pH solution (e.g., 2.0), the film swells dramatically to more than 6 times its original thickness, as measured by *in situ* ellipsometry (Figure 4a, thickness ~1300 nm and $n_f = 1.34$). Nanotubes, as observed by CLSM (Figure 6b), also undergo this dramatic swelling transition. The dramatic swelling of the PAH7.5/PAA3.5 multilayer is due to the breakage of $\text{NH}_3^+ - \text{COO}^-$ ionic cross-links as a result of the protonation of the carboxylate groups from PAA (state A, Scheme 3) and is further driven by osmotic forces and charge repulsion among the free, positively charged amine groups generated from the breakage of the ionic cross-links. We recently reported that this highly swollen state exhibits a high capacity to bind negatively charged gold complexes as a result of the abundance of free, positively charged amine groups⁴⁰ created when the acid groups become protonated. Upon drying (path 4), the multilayer collapses to a dense structure (state C, thickness = ca. 170 nm, $n_f = 1.53$). The decrease in film thickness relative to the as-prepared film indicates a slight loss of material during this initial low-pH treatment. However, after the first low-pH treatment, the dry film thickness measured after subsequent low-pH immersions remains essentially constant (results not shown).

If the highly swollen film (in a low-pH solution) is immersed in a higher-pH solution (≥ 5.5) without drying (path 1), then the extent of swelling of the film decreases as carboxylate-based ionic cross-links are regenerated (state B, thickness = 690 nm, $n_f = 1.36$). The reformation of these ionic cross-links, however, does not reestablish the low swelling level of the as-assembled multilayer, suggesting that the molecular reorganization induced by the first

acid treatment has irreversibly altered the multilayer organization. This latter process of reforming ionic cross-links results in the rejection of water from the previously very highly swollen network (microsyneresis). Because this water rejection process occurs in a spatially inhomogeneous fashion, micrometer- (or smaller) sized pockets of water are formed and trapped within the new, tighter network structure. When this structure dries, it leaves pores (air pockets) where the water pockets used to be. An accompanying spinodal-like phase-separation process may also be in play and cannot be ruled out at this point. The spatially inhomogeneous multilayer organization, when dried (path 2), gives rise to the nanoporous film (state D, thickness = 230 nm, $n_f = 1.37$). Exposing the multilayer film from either the dry state or the pH 5.5 wet state to a pH 2.0 environment essentially erases the nanoheterogeneous structure and reestablishes a highly swollen, more homogeneous state (state A).

If the highly swollen film (in a low-pH solution) is dried (state C) and then immersed in a higher-pH solution (≥ 5.5), then the film initially swells to a high level (within seconds) followed by a deswelling process (in minutes) (Supporting Information). Thus, the free ammonium groups present in the dried film (previously formed in the low-pH highly swollen state) lead to the initial high swelling level of the film. However, because the higher-pH solution deprotonates carboxylic acid groups from PAA to carboxylates and reforms carboxylate-based ionic linkages, this high level of swelling is quickly followed by deswelling into the heterogeneous state previously described (state B). The rate and extent of swelling in both stages are expected to be strongly dependent on the kinetics of three factors: osmotic forces, charge repulsion, and ionic cross-linking.

The above mechanism accounts for all of the observations made with the PAH7.5/PAA3.5 and PAH8.6/PAA3.5 multilayers driven to the nanoporous state. In the above scenario, after the initial acid treatment, a water rinse at a higher pH is needed to reform ionic cross-links and induce microsyneresis. In the case of

the microporous transition, however, porosity can be produced in the dry state by treating the film at pH 2.5 without a subsequent higher-pH water rinse.³⁸ At pH 2.5, a smaller number of ionic cross-links are broken (Figure 4a), apparently resulting in the formation of a microheterogeneous state in the low-pH solution.

Conclusions

An understanding of the pH-triggered molecular rearrangements in PAH7.5/PAA3.5 multilayers led to the design and synthesis of submicrometer-sized reversibly swellable PEM tube arrays. The reversible swelling–deswelling transition of the PEM nanotube arrays, observed directly by significant changes in the nanotube dimensions, was further utilized to actuate the simple movement of surface-bound colloidal particles. Aided by previous studies, in situ characterization of the PAH7.5/PAA3.5 multilayers in the form of substrate-attached nanotube arrays provided a more in-depth understanding of the molecular

reconfigurations occurring during the swelling–deswelling transition in solution and the resultant effects on the molecular architecture and physical properties of dry films.

Acknowledgment. This work was supported by the MRSEC Program of the National Science Foundation under grant number DMR 08-19762. We thank the Center for Materials Science and Engineering (CMSE) and the Institute of Soldier Nanotechnologies (ISN) for the use of characterization equipment and Ms. Erin Goodwin of Roxbury Community College for experimental contributions.

Supporting Information Available: In situ ellipsometry measurements of film thickness of a $(\text{PAH7.5}/\text{PAA3.5})_{20}$ PEM on a planar substrate during and after different pH treatments. This material is available free of charge via the Internet at <http://pubs.acs.org>.